

Study of N^* Production from $J/\psi \rightarrow p\bar{p}\eta$

J. Z. Bai¹, Y. Ban⁶, J. G. Bian¹, J. F. Chang¹, A. D. Chen¹, H. F. Chen², H. S. Chen¹,
J. C. Chen¹, X. D. Chen¹, Y. B. Chen¹, B. S. Cheng¹, S. P. Chi¹, Y. P. Chu¹, X. Z. Cui¹,
Y. S. Dai⁴, L. Y. Dong¹, Z. Z. Du¹, H. Y. Fu¹, L. P. Fu¹², C. S. Gao¹, S. D. Gu¹, Y. N. Guo¹,
Z. J. Guo¹, S. W. Han¹, Y. Han¹, J. He¹, J. T. He¹, K. L. He¹, M. He³, X. He¹, T. Hong¹,
Y. K. Heng¹, G. Y. Hu¹, H. M. Hu¹, Q. H. Hu¹, T. Hu¹, G. S. Huang⁸, X. P. Huang¹,
Y. Z. Huang¹, X. B. Ji³, C. H. Jiang¹, Y. Jin¹, Z. J. Ke¹, Y. F. Lai¹, D. Li¹, H. B. Li¹,
H. H. Li⁷, J. Li¹, J. C. Li¹, P. Q. Li¹, Q. J. Li¹, R. Y. Li¹, W. Li¹, W. G. Li¹, X. N. Li¹,
X. Q. Li⁹, B. Liu¹, F. Liu⁷, Feng Liu¹, H. M. Liu¹, J. Liu¹, J. P. Liu¹¹, T. R. Liu¹,
R. G. Liu¹, Y. Liu¹, Z. X. Liu¹, G. R. Lu¹⁰, F. Lu¹, J. G. Lu¹, Z. J. Lu¹, X. L. Luo¹,
E. C. Ma¹, F. C. Ma¹³, J. M. Ma¹, Z. P. Mao¹, X. C. Meng¹, X. H. Mo¹, J. Nie¹, Z. D. Nie¹,
N. D. Qi¹, X. R. Qi⁶, C. D. Qian⁵, J. F. Qiu¹, Y. K. Que¹, G. Rong¹, Y. Y. Shao¹,
B. W. Shen¹, D. L. Shen¹, H. Shen¹, X. Y. Shen¹, H. Y. Sheng¹, F. Shi¹, H. Z. Shi¹,
X. F. Song¹, H. S. Sun¹, L. F. Sun¹, Y. Z. Sun¹, S. Q. Tang¹, X. Tang¹, G. L. Tong¹,
J. Wang¹, J. Z. Wang¹, L. Wang¹, L. S. Wang¹, M. Wang¹, Meng Wang¹, P. Wang¹,
P. L. Wang¹, S. M. Wang¹, W. F. Wang³, Y. Y. Wang¹, Z. Y. Wang¹, C. L. Wei¹, N. Wu¹,
D. M. Xi¹, X. M. Xia¹, X. X. Xie¹, G. F. Xu¹, Y. Xu¹, S. T. Xue¹, M. L. Yan², W. B. Yan¹,
W. G. Yan¹, C. M. Yang¹, C. Y. Yang¹, G. A. Yang¹, H. X. Yang¹, X. F. Yang¹, M. H. Ye⁸,
S. W. Ye², Y. X. Ye², C. S. Yu¹, C. X. Yu¹, G. W. Yu¹, Y. Yuan¹, Y. Zeng¹², B. Y. Zhang¹,
C. C. Zhang¹, D. H. Zhang¹, H. L. Zhang¹, H. Y. Zhang¹, J. Zhang¹, J. W. Zhang¹,
L. Zhang¹, L. S. Zhang¹, P. Zhang¹, Q. J. Zhang¹, S. Q. Zhang¹, X. Y. Zhang³, Y. Y. Zhang¹,
Z. P. Zhang¹, D. X. Zhao¹, H. W. Zhao¹, Jiawei Zhao², J. W. Zhao¹, P. P. Zhao¹,
W. R. Zhao¹, Y. B. Zhao¹, Z. G. Zhao¹, J. P. Zheng¹, L. S. Zheng¹, Z. P. Zheng¹,
X. C. Zhong¹, B. Q. Zhou¹, G. M. Zhou¹, L. Zhou¹, K. J. Zhu¹, Q. M. Zhu¹, Y. C. Zhu¹,
Y. S. Zhu¹, Z. A. Zhu¹, B. A. Zhuang¹, B. S. Zou¹

(BES Collaboration)[†]

H.C.Chiang,¹ G.X.Peng,¹ J.X.Wang,¹ J.J.Zhu,²

¹ *Institute of High Energy Physics, Beijing 100039, People's Republic of China*

² *University of Science and Technology of China, Hefei 230026, People's Republic of China*

³ *Shandong University, Jinan 250100, People's Republic of China*

⁴ *Hangzhou University, Hanzhou 310028, People's Republic of China*

⁵ *Shanghai Jiaotong University, Shanghai 200030, People's Republic of China*

⁶ *Peking University, Beijing 100871, People's Republic of China*

⁷ *Hua Zhong Normal University, Wuhan 430079, People's Republic of China*

⁸ *China Center for Advanced Science and Technology(CCAST), World Laboratory, Beijing 100080, People's Republic of China*

⁹ *Nankai University, Tianjin 300071, People's Republic of China*

¹⁰ *Henan Normal University, Xinxiang 453002, People's Republic of China*

¹¹ *Wuhan University, Wuhan 430072, People's Republic of China*

¹² *Hunan University, Changsha 410082, People's Republic of China*

¹³ *Liaoning University, Shenyang 110036, People's Republic of China*

Data are presented on the reaction $J/\psi \rightarrow p\bar{p}\eta$ using $7.8 \times 10^6 J/\psi$ triggers collected by the BEJing Spectrometer (BES). A partial wave analysis is performed. A clear enhancement near the $p\eta(\bar{p}\eta)$ threshold is observed. It is fitted with a $J^P = \frac{1}{2}^-$ resonance with mass $M = 1530 \pm 10$ MeV and width $\Gamma = 95 \pm 25$ MeV. In addition, there is a peak around 1650 MeV with $J^P = \frac{1}{2}^-$ preferred also, fitted with $M = 1647 \pm 20$ MeV and $\Gamma = 145^{+80}_{-45}$ MeV. These two N^* resonances are

believed to be the two well established states, $S_{11}(1535)$ and $S_{11}(1650)$, respectively. It is the first partial wave study of the production of these resonances from J/ψ decays.

PACS: 13.25.Gv; 14.20Gk; 13.65.+i

I. INTRODUCTION

Nucleons are the most common form of hadronic matter on the earth and probably in the whole universe. To understand the internal quark-gluon structure of nucleon and its excited states N^* 's is one of the most important tasks in nowadays particle and nuclear physics. The main source of information for the nucleon internal structure is their mass spectrum, various production and decay rates. Our present knowledge on this aspect came almost entirely from the old generation of πN experiments of more than twenty years ago [1]. Considering its importance for the understanding of the nonperturbative QCD [2], a new generation of experiments on N^* physics with electromagnetic probes (real photon and space-like virtual photon) has recently been started at new facilities such as CEBAF at JLAB, ELSA at Bonn, GRAAL at Grenoble.

The J/ψ experiment at the Beijing Electron-Positron Collider(BEPC) has long been known as the best place for looking for glueballs. But in fact it is also an excellent place for studying N^* resonances [3], especially in the mass range 1-2 GeV. The corresponding Feynman graphs for the N^* and \bar{N}^* production are shown in Fig. 1. These graphs are almost identical to those describing the N^* electro-production process if the direction of the time axis is rotated by 90° . The only difference is that the virtual photon here is time-like instead of space-like and couples to NN^* through a real vector charmonium meson J/ψ . Therefore almost all channels of N^* decays studied at the CEBAF and other $\gamma p(ep)$ facilities can also be studied here.

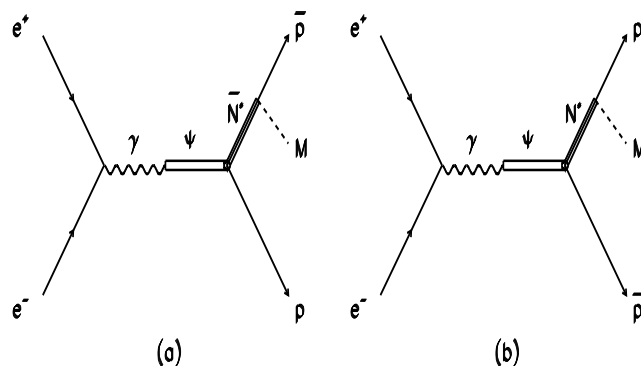


FIG. 1. Feynman graphs for N^* and \bar{N}^* production from e^+e^- collision through J/ψ meson

Among many interesting channels, the $J/\psi \rightarrow p\bar{p}\eta$ is a relatively simple one to begin with. According to the information [1,4–6] from $\pi N \rightarrow \eta N$ and $\gamma N \rightarrow \eta N$ experiments, as well as some early quark shell model calculation [7], only $N^*(1535)S_{11}$ has a big decay branching

ratio to $N\eta$, while $N^*(1650)S_{11}$ may have a branching ratio to $N\eta$ of up to 10% and other N^* resonances below 2.0 GeV have much smaller branching ratios to the $N\eta$.

In this paper, we present BES data and a partial wave analysis on the $J/\psi \rightarrow p\bar{p}\eta$ reaction. The $N^*(1535)$ and $N^*(1650)$ are observed. This is the first partial wave study of the production of these N^* resonances from the J/ψ hadronic decays in the world. The new information on $J/\psi NN^*$ couplings provides a new source for studying baryon structure [8].

II. BES DETECTOR

The analysis in this paper uses 7.8×10^6 J/ψ triggers collected by the Beijing Spectrometer(BES). BES is a conventional solenoidal magnet detector that is described in detail in Ref. [9]. A four-layer central drift chamber(CDC) surrounding the beampipe provides trigger information. A forty-layer cylindrical main drift chamber(MDC), located radially outside the CDC, provides trajectory and energy loss (dE/dX) information for charged tracks over 85% of the total solid angle. The momentum resolution is $\sigma_P/P = 0.017\sqrt{1+P^2}$ (p in GeV/c), and the dE/dX resolution for hadron tracks is 11%. An array of 48 scintillation counters(with inner radius of 1.157 meter and outer radius 1.207 meter)surrounding the MDC measures the time-of-flight(TOF) of charged tracks with a resolution of 450 ps for hadrons. Radially outside of TOF system is a 12 radiation length thick, lead-gas barrel shower counter(BSC) operating in the limited streamer mode. This device covers 80% of the total solid angle and measures the energies of electrons and photons with an energy resolution of $\sigma_E/E = 22\%/\sqrt{E}$ (E GeV). Outside the BSC is a solenoid, which provides a 0.4 Tesla magnetic field over the tracking volume. An iron flux return is instrumented with three double layers of counters that identify muons of momentum greater than 0.5 GeV/C.

III. EVENT SELECTION

The η is detected here in its $\gamma\gamma$ decay mode. Therefore, much effort has been devoted to the selection of the events in the $2\gamma p\bar{p}$ final state. Each candidate event is required to have two oppositely signed charged tracks with a good helix fit in the polar angle range $-0.8 < \cos\theta < 0.8$ in MDC and at least 2 reconstructed γ 's in BSC. A vertex is required within an interaction region ± 15 cm longitudinally and 2 cm radially. A minimum energy cut of 60 MeV is imposed on the photons. Showers associated with charged tracks are also removed.

After above selection, we use TOF information to identify the $p\bar{p}$ pairs, and at least one track with unambiguous TOF information is required. The open angle of two charged tracks smaller than 175° is required in order to remove back to back events; to remove radiative Bhabha events, we require $(E_+/P_+ - 1)^2 + (E_-/P_- - 1)^2 > 0.3$, where E_+ , P_+ (E_- , P_-) are the energy deposited in BSC and momentum of positron (electron) respectively. Events are fitted kinematically to the 4C hypotheses $J/\psi \rightarrow 2\gamma p\bar{p}$. If the number of the selected photons is larger than two, the fit is repeated using all permutations of the photons. For events with a good fit, the two photon combination with the largest probability is selected. Fig. 2 shows the invariant mass spectrum of two gammas, we can see clear π^0 and η signals. Meanwhile, the events are also fitted to $J/\psi \rightarrow \gamma p\bar{p}$ and $4\gamma p\bar{p}$. We require

$$Prob(\chi^2_{(2\gamma p\bar{p})}, 4C) > Prob(\chi^2_{(\gamma p\bar{p})}, 4C), \quad Prob(\chi^2_{(2\gamma p\bar{p})}, 4C) > Prob(\chi^2_{(4\gamma p\bar{p})}, 4C)$$

to reject the $\gamma p\bar{p}$ and $p\bar{p}\pi^0\pi^0$ backgrounds. In order to suppress further the backgrounds with a π^0 , a 5C fit for the $p\bar{p}\eta$ with $\eta \rightarrow \gamma\gamma$ is performed on the selected events. $Prob(\chi^2_{p\bar{p}\eta}, 5C) > 1\%$ is required. This 5C fit helps improving the mass resolution for combinations of charged particles. There are 765 events which survive our selections.

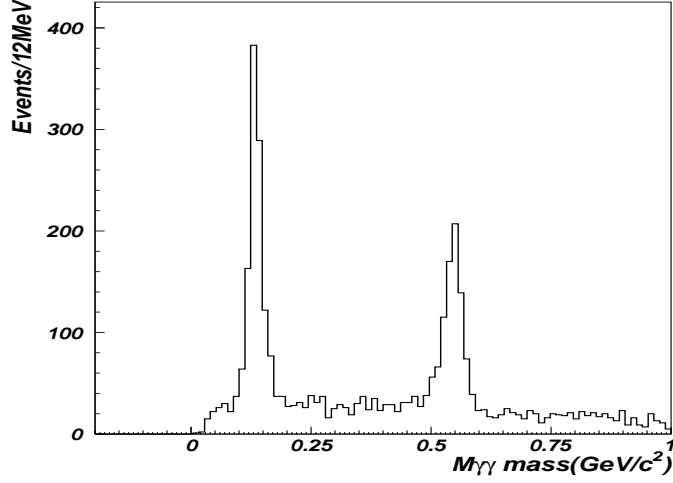


FIG. 2. $\gamma\gamma$ invariant mass spectrum after 4C fit for $J/\psi \rightarrow p\bar{p}\gamma\gamma$

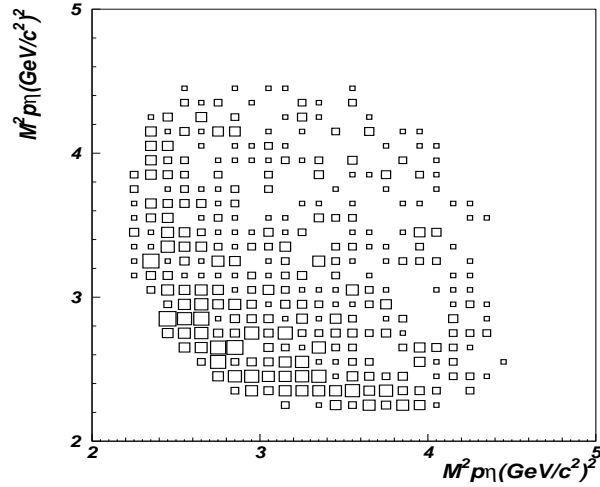


FIG. 3. Dalitz plot for $J/\psi \rightarrow p\bar{p}\eta$ ($M_{p\eta}^2$ v $M_{\bar{p}\eta}^2$)

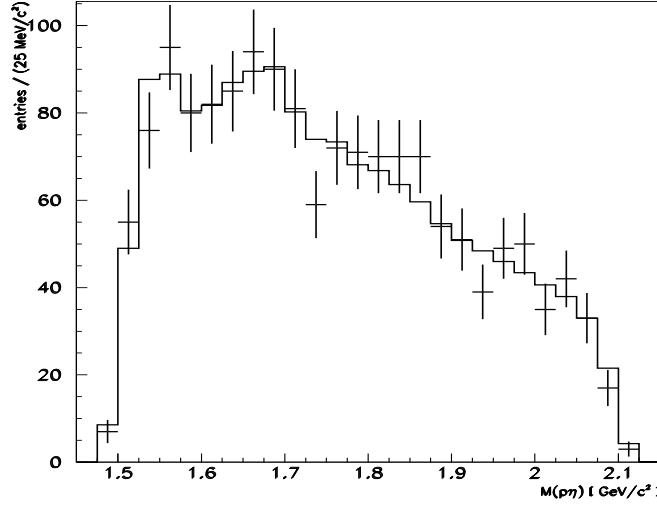


FIG. 4. $p\eta(\bar{p}\eta)$ invariant mass spectrum for $J/\psi \rightarrow p\bar{p}\eta$, crosses are data and histogram the fit

Fig. 3 is the Dalitz plot for the decay $J/\psi \rightarrow p\bar{p}\eta$. The corresponding $p\eta(\bar{p}\eta)$ invariant mass spectrum is shown in Fig. 4. There is a clear enhancement near the $p\eta(\bar{p}\eta)$ threshold. There are also some bumps around 1.65 GeV and 1.8 GeV.

IV. SIMULATION OF SIGNALS AND BACKGROUNDS

In order to estimate the selection efficiency, a phase space generator is used to produce a sample of $p\bar{p}\eta$ events with full detector simulation, it is 18% after the Monte Carlo data go through the same cuts as real data.

Since $2\gamma p\bar{p}$ is the final state of the reaction channel, the possible background may come from $J/\psi \rightarrow p\bar{p}\pi^0$, $p\bar{p}\pi^0\pi^0$, $p\bar{p}\omega$, $\pi^+\pi^-\pi^0$ and $K^+K^-\pi^0$ decay modes. For each channel, 10,000 MC events are generated. These MC events go through the same analysis program as for the real data. We find that only $p\bar{p}\pi^0\pi^0$ channel gives a significant contribution to the background. The estimated background is 8%,

A correct estimation of the background invariant mass shape is essential to the partial wave analysis. Fortunately, the invariant mass spectrum of these events is of the same shape as the $J/\psi \rightarrow p\bar{p}\eta$ phase space distribution. Fig. 5 shows the mass distributions of the background from $J/\psi \rightarrow p\bar{p}\pi^0\pi^0$, compared with the phase space distribution for the $J/\psi \rightarrow p\bar{p}\eta$ process from Monte Carlo data. A side-band method is also used to check the shape of possible backgrounds from real data; the same result is obtained.

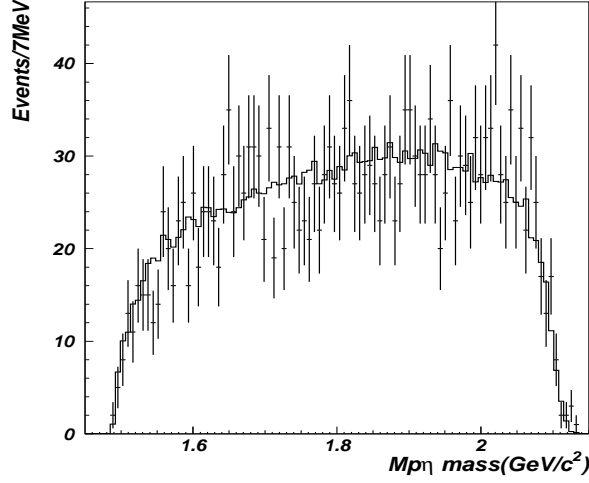


FIG. 5. The $p\eta$ invariant mass distribution of the background from $J/\psi \rightarrow p\bar{p}\pi^0\pi^0$ channel (crosses), compared with the phase-space distribution for the $J/\psi \rightarrow p\bar{p}\eta$ reaction (histograms)

V. AMPLITUDE ANALYSIS

Based on the study of $p\bar{p}$ and $p\eta$ invariant mass distributions in our data, we are mainly interested in the structures at 1535 and 1650 MeV of the $p\eta$ invariant mass. According to PDG [1], below 1900 MeV there are eight N^* resonances observed by other experiments, *i.e.*, $P_{11}(1440)$, $S_{11}(1535)$, $S_{11}(1650)$, $D_{15}(1675)$, $F_{15}(1680)$, $D_{13}(1700)$, $P_{11}(1710)$ and $P_{13}(1720)$ states, among which only $S_{11}(1535)$ and $S_{11}(1650)$ were observed in the ηN decay mode. Although the two $p\eta$ structures at 1535 and 1650 MeV in our data are most probably due to $S_{11}(1535)$ and $S_{11}(1650)$ states, we perform the partial wave analysis by allowing all possible quantum numbers of $J^P = \frac{1}{2}^{\pm}$, $\frac{3}{2}^{\pm}$ and $\frac{5}{2}^{\pm}$.

The background from multi- π^0 is $\sim 8\%$ in the 5C fit. We have included a phase space background in the PWA fit to allow for this.

In this analysis, we use the effective Lagrangian approach for the partial wave analysis. The relevant spin-1/2 interaction Lagrangians are [11,12]

$$\mathcal{L}_{\eta PR}^1 = -ig_{\eta PR}\bar{P}\Gamma R\eta + H.c., \quad (1)$$

$$\mathcal{L}_{\psi PR}^{(1)} = \frac{ig_{T_R}}{M_R + M_P}\bar{R}\Gamma_{\mu\nu}q^\nu P\psi^\mu + H.c., \quad (2)$$

$$\mathcal{L}_{\psi PR}^{(2)} = -g_{V_R}\bar{R}\Gamma_\mu P\psi^\mu + H.c. \quad (3)$$

where R is the generic notation for the resonance with mass M_R , P for proton with mass M_P and ψ for J/ψ with four-momentum q . The vertex coupling constants $g_{\eta PR}$, g_{T_R} and g_{V_R} are parameters to be determined by fitting experimental data. Note here from the single $\bar{p}p\eta$ channel, we can only determine products of coupling constants, *i.e.*, $g_{\eta PR}g_{T_R}$ and $g_{\eta PR}g_{V_R}$. The operator structures for the Γ , Γ_μ and $\Gamma_{\mu\nu}$ are

$$\Gamma = 1, \quad \Gamma_\mu = \gamma_5\gamma_\mu, \quad \Gamma_{\mu\nu} = \gamma_5\sigma_{\mu\nu}, \quad (4)$$

$$\Gamma = \gamma_5, \quad \Gamma_\mu = \gamma_\mu, \quad \Gamma_{\mu\nu} = \sigma_{\mu\nu}, \quad (5)$$

where (4) and (5) correspond to nucleon resonances of $J^P = \frac{1}{2}^-$ and $\frac{1}{2}^+$, respectively. The interaction Lagrangians for $J^P = \frac{3}{2}^\pm$ and $\frac{5}{2}^\pm$ N^* resonances are constructed similarly [13]. The amplitudes in the PWA analysis are constructed from these Lorentz-invariant interactions and the N^* propagators [14] for J/ψ initial states with helicity ± 1 . The relative magnitudes and phases of the amplitudes are determined by a maximum likelihood fit to the data. The BW parameters for different states are fitted. The $p\eta$ mass projection fitted to the real data is shown in Fig. 4. Fig. 6 shows the data and fit for the polar angle of the proton measured with respect to the beam direction. Fig. 7 shows the invariant mass spectra for $p\bar{p}$. We now discuss the features of the data and the outcome of fits.

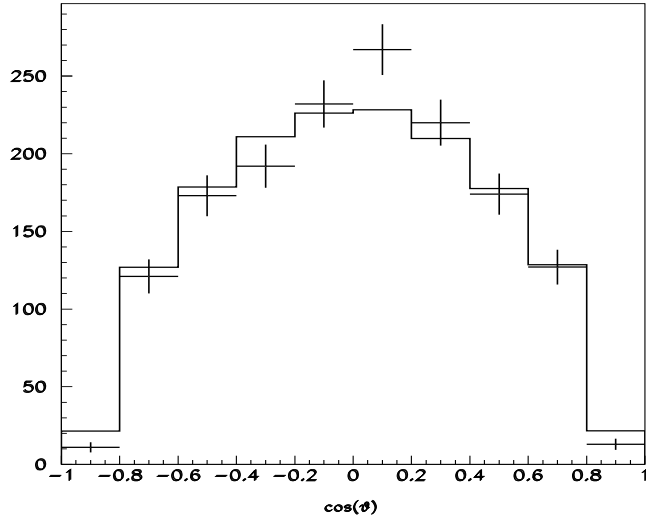


FIG. 6. The polar angle of proton measured with respect to the beam direction, crosses are data and histograms the fit

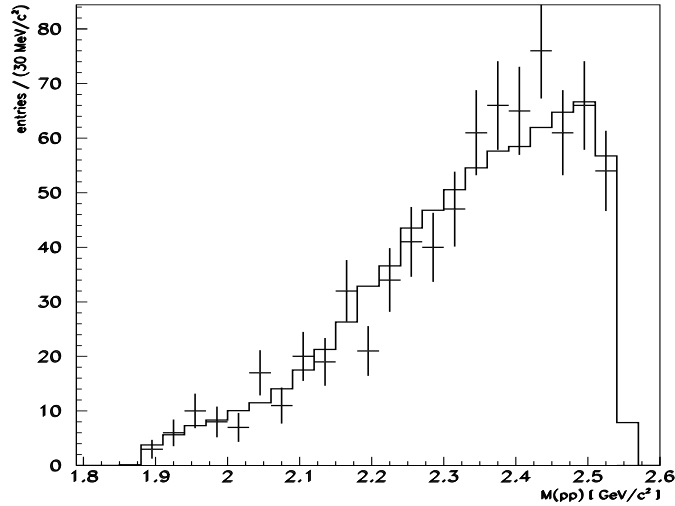


FIG. 7. $p\bar{p}$ invariant mass spectra for $J/\psi \rightarrow p\bar{p}\eta$, crosses are data and histograms the fit

$S_{11}(1535)$

The peak around 1535 MeV near the $p\eta$ threshold optimizes at $M = 1530 \pm 10$ MeV and $\Gamma = 95 \pm 15$ MeV. The data favour $J^P = \frac{1}{2}^-$ over others. A fit with $J^P = \frac{1}{2}^+$ instead gives $\ln L$ worse by 7.5 than for $\frac{1}{2}^-$ assignment (Our definition of $\ln L$ is such that it increases by 0.5 for a one standard deviation change in one parameter). Fits with other quantum numbers are much worse, *e.g.*, $\ln L$ worse by 26 for $J^P = \frac{3}{2}^-$. With our 4 fitted parameters, the statistical significance of the peak is above 6.0σ . It is obviously the $S_{11} N^*(1535)$ resonance. It makes the largest contribution $(56 \pm 15)\%$ to the $p\bar{p}\eta$ final states, the errors here and later include both statistics and systematic errors from the fit. Our results for $N^*(1535)$ are consistent with the resonance parameters of PDG [1] and a recent detailed analysis of πN S_{11} partial wave by Vrana, Dytman and Lee [15].

$S_{11}(1650)$

The second peak around 1650 MeV is also fitted with a $J^P = \frac{1}{2}^-$ resonance $N^*(1650)$. It optimizes at $M = 1647 \pm 20$ MeV, $\Gamma = 145^{+80}_{-45}$ MeV, and contributes $(24^{+5}_{-15})\%$ to the $p\bar{p}\eta$ final states. We have tried fits to this peak with other quantum numbers. The log likelihood is worse by 3, 4, 5, 6, 12 for $\frac{5}{2}^+$, $\frac{3}{2}^+$, $\frac{5}{2}^-$, $\frac{1}{2}^+$ and $\frac{3}{2}^-$, respectively. Note there are two more free parameters for $J^P = \frac{3}{2}^\pm$ and $J^P = \frac{5}{2}^\pm$ modes than for $J^P = \frac{1}{2}^\pm$ modes. If we assume no contribution from resonance around 1650 MeV, then the mass and width of $S_{11}(1535)$ optimize around 1570 MeV and 270 MeV, respectively, which are out of the range of PDG values. The log likelihood is worse by 14.

A small improvement to the fit is given by including a $J^P = \frac{1}{2}^+$ resonance, which optimizes at $M = 1800 \pm 40$ MeV and $\Gamma = 165^{+165}_{-85}$ MeV. It contributes $(12 \pm 7)\%$ to the $p\bar{p}\eta$ final states. The statistical significance of the peak is only 2.0σ . We have tried other quantum numbers. All of them give equally good fits within one standard deviation. There is a theoretical prediction [10] that the lowest-lying hybrid states should be around this energy region.

We also include a small contribution $(8 \pm 4)\%$ from the tail of $P_{11}(1440)$ resonance with its mass and width fixed to its PDG central values for its pole position [1]. It is also only a 2.0σ effect.

Fig. 8 shows the different component contribution.

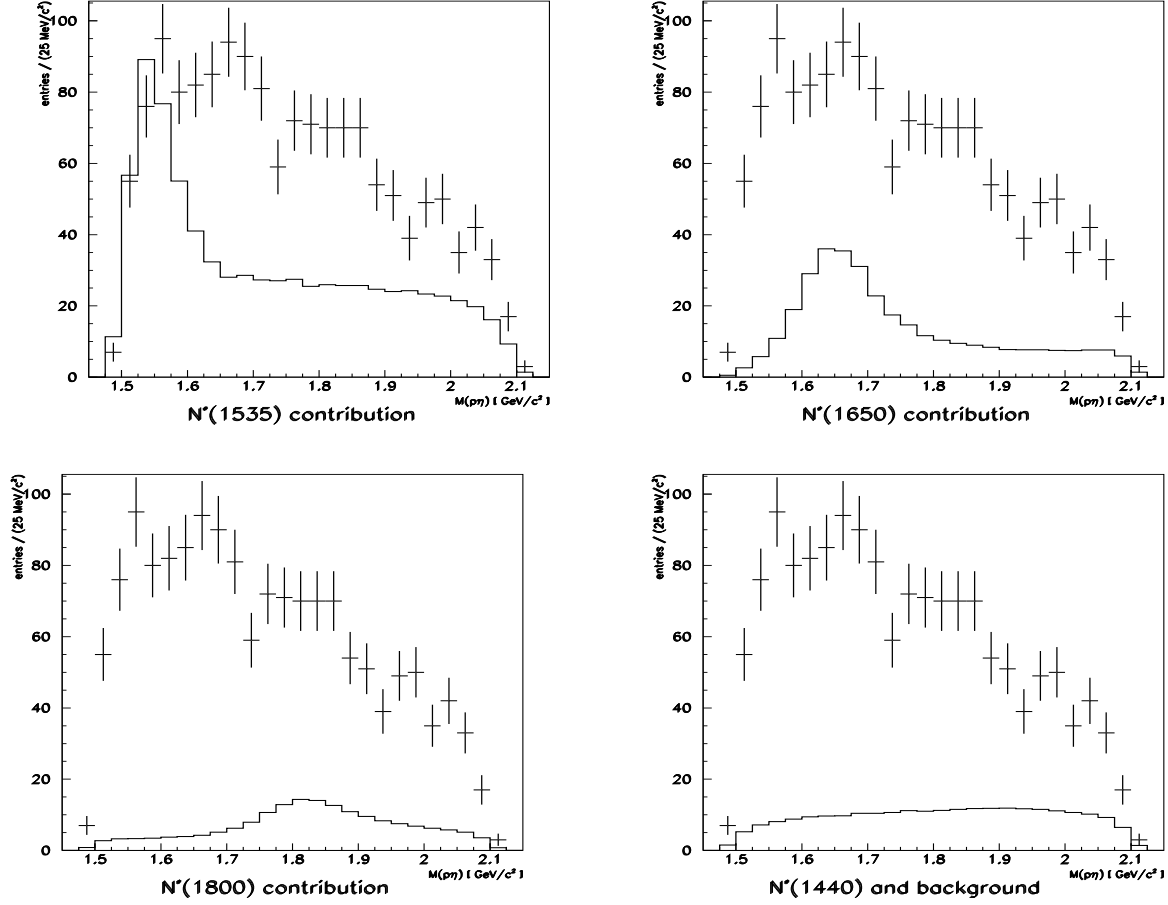


FIG. 8. Component contribution

An interesting result is that the $\mathcal{L}_{\psi PR}^{(2)}$ term given by Eq.(3) makes insignificant contribution for both $S_{11}(1535)$ and $S_{11}(1650)$. If we drop this kind of couplings for both resonances, the likelihood value for the fit is only worse by 0.9 for 4 less free parameters. This kind of couplings should vanish for the real photon coupling to NN^* due to the requirement of the gauge invariance. Why it also vanishes for the ψNN^* coupling needs to be understood. A theoretical calculation [16] assuming pure $\mathcal{L}_{\psi PR}^{(2)}$ coupling without $\mathcal{L}_{\psi PR}^{(1)}$ coupling failed to reproduce the basic feature of the $J/\psi \rightarrow \bar{p}p\eta$ data. This is consistent with our observation that the $\mathcal{L}_{\psi PR}^{(1)}$ coupling dominates for both $N^*(1535)$ and $N^*(1650)$.

In the Vector Meson Dominance (VMD) picture, the virtual photon couples to the NN^* through vector mesons, and the electro-magnetic NN^* transition form factors $g_{\gamma^* NN^*}$ can be expressed in terms of photon-meson coupling strengths $C_{\gamma V}$ and meson- NN^* vertex form factors $g_{Vj NN^*}$:

$$g_{\gamma^* NN^*}(q^2) = \sum_j \frac{m_j^2 C_{\gamma V_j}}{m_j^2 - q^2 - im_j \Gamma_j} g_{V_j NN^*}(q^2) \quad (6)$$

with

$$C_{\gamma V} = \sqrt{\frac{3\Gamma_{V \rightarrow e^+e^-}}{\alpha m_V}}. \quad (7)$$

At $q^2 = M_\psi^2$, the J/ψ meson dominates. The terms from other vector mesons are negligible.

From our PWA results here and other relevant information from PDG [1], we can deduce the transition form factor for the time-like virtual photon to $PN^*(1535)$ as

$$|g_{\gamma^* p N^*}(q^2 = M_\psi^2)| = 2.3 \pm 0.5, \quad (8)$$

which is related to the more familiar helicity amplitude $A_{1/2}^P$ for $N^* \rightarrow \gamma P$ by

$$|A_{1/2}^P|^2 = \left(\frac{g_{\gamma p N^*}(q^2 = 0)}{M_{N^*} + M_P} \right)^2 \frac{(M_{N^*}^2 - M_P^2)}{2M_P}. \quad (9)$$

This is the first measurement of the form factor $g_{\gamma^* p N^*}$ for a time-like virtual photon. It provides a new challenge for various theoretical models to reproduce it, complementary to the information for a real or space-like virtual photon [17].

VI. CONCLUSION

In summary, the J/ψ decay at BEPC provides a new excellent laboratory for studying the N^* resonances. We have studied the $J/\psi \rightarrow p\bar{p}\eta$ decay channel, and a PWA analysis is performed on the data. There is a definite requirement for a $J^P = \frac{1}{2}^-$ component at $M = 1530 \pm 10$ MeV with $\Gamma = 95 \pm 25$ MeV near the ηN threshold. In addition, there is an obvious resonance around 1650 MeV with $J^P = \frac{1}{2}^-$ preferred, $M = 1647 \pm 20$ MeV and $\Gamma = 145^{+80}_{-45}$ MeV. In the higher $p\eta(\bar{p}\eta)$ mass region, there is an evidence for a structure around 1800 MeV; with present statistics we cannot determine its quantum numbers.

All above analysis is the first step for us to probe N^* baryons at BES. We will perform a detail study of N^* baryons in the following J/ψ decay channels: $J/\psi \rightarrow p\bar{p}\pi^0$, $p\bar{n}\pi^-$, $p\bar{p}\pi^0\pi^0$, $p\bar{p}\pi^+\pi^-$, $p\bar{p}\eta'$, $p\bar{p}\omega$ and so on.

With the forthcoming 50 million more J/ψ events in near future, more precise partial wave analyses can be carried out on many channels involving N^* resonances and should offer some determinations of N^* properties. A systematic experimental study of the N^* production from the J/ψ decays is underway and will provide a new domain to explore the internal quark-gluon structure of these excited nucleons.

VII. ACKNOWLEDGEMENTS

We thank D.V.Bugg, S.Dytman, L.Kisslinger, P.R.Page and P.Stoler for useful discussions, and the staff of IHEP for technical support in running the experiment. This work is partly supported by China Postdoctoral Science Foundation and National Science Foundation of China under contract Nos. 19290401, 19605007, 19991487 and 19905011; and by the Chinese Academy of Sciences under contract No. KJ 95T-03(IHEP)

[†] Data analyzed were taken prior to the participation of U.S. members of the BES Collaboration.

[1] Particle Data Group, Eur. Phys. J. C15 (2000) 1.

- [2] N.Isgur and G.Karl, Phys. Rev. D **18** (1978) 4187; *ibid.* **19** (1979) 2653;
S.Capstick and N.Isgur, Phys. Rev. D **34** (1986) 2809;
R.Bijker, F.Iachello and A.Leviathan, Ann. Phys. (N.Y.) **236** (1994) 69;
K.F.Liu and C.W.Wong, Phys. Rev. D (1983) 170.
- [3] B.S.Zou, Talks at CCAST workshop on BES Future Physics, Aug. 1998, CCAST-WL Workshop Series: Volume 117 (2000) 69; Nucl. Phys. A **675** (2000) 197c.
- [4] B. Krusche, *et al.*, Phys. Rev. Lett. **74**(1995)3736.
- [5] M.Benmerrouche and N.C. Mukhopadhyay, Phys. Rev. Lett. **67**(1991)1070;
M.Benmerrouche, N.C. Mukhopadhyay and J-F. Zhang, Phys. Rev.D **51**(1995)3237.
- [6] M.Batinic, I.Slaus and A.Svarc, *Phys. Rev. C* **51** (1995) 2310; A.M.Green and S.Wycech, *Phys. Rev. C* **60** (1999) 035208.
- [7] A.Mitra, Phys. Lett. B **51**(1974)149.
- [8] B.S.Zou et al., Preprint hep-ph/9909204.
- [9] BES Collaboration, Nucl. Instr. Methods, **A344**(1994)319.
- [10] Simon Capstick, Philip R. Page, *Phys. Rev. D* **60** (1999) 111501.
- [11] M.Benmerrouche, N.C.Mukhopadhyay and J.F.Zhang, *Phys. Rev. Lett.* **77** (1996) 4716; *Phys. Rev. D* **51** (1995) 3237.
- [12] M.G.Olsson and E.T.Osypowski, *Nucl. Phys. B* **87** (1975) 399; *Phys. Rev. D* **17** (1978) 174;
M.G.Olsson et al., *ibid.* **17** (1978) 2938.
- [13] W.Rarita and J.Schwinger, Phys. Rev. **60** (1941) 61.
- [14] C.Fronsdal, Nuovo Cimento Suppl. **9** (1958) 416; R.E.Behrends and C.Fronsdal, Phys. Rev. **106** (1957) 345.
- [15] T.P.Vrana, S.A.Dytman and T.S.H.Lee, PR **328** (2000) 181.
- [16] R. Sinha and S. Okubo, *Phys. Rev. D* **30** (1984) 2333.
- [17] G.Sterman and P.Stoler, Ann. Rev. Nucl. Part. Sci. **43** (1997) 193.